Theor Chem Acc (2007) 117: 127–135
DOI 10.1007/s00214-006-0155-8

REGULAR ARTICLE

Alain Berthod · John J. Kozak · Jared L. Anderson
Jie Ding · Daniel W. Armstrong

Ionic liquid-alkane association in dilute solutions

Received: 2 December 2005 / Accepted: 19 May 2006 / Published online: 13 July 2006

Abstract Enthalpies and entropies of transfer were measured by gas chromatography for dilute solutions of a homologous series of eight even *n*-alkanes (from octane to docosane) into six different ionic liquids (ILs) (namely, 1-butyl-3-methylimidazolium chloride, bromide, iodide, triflate and hexafluorophosphate; plus *N*-butylmethylpyridinium *bis* {(trifluoromethyl) sulfonyl}-imide) over the 80–150 °C temperature range, all ILs being in the liquid state. Over a narrow concentration range, the entropic change may be consistent with a solvophobic association model of *n*-alkanes in ILs. A very simple model is proposed to account for the thermodynamic data. This approach can be used to approximate interionic distances and possible dielectric constants for ILs. Although the model may have some use in dilute alkane-IL solutions, more sophisticated models, particularly for the enthalpic contributions, are desirable.

Keywords Molten salts · Ionic liquid · Thermodynamics · Hydrophobic association · Alkanes

1 Introduction

The basis for a growing, widespread interest in room temperature ionic liquids (RTILs) is the combination of their broad solvation abilities coupled with other unusual and useful properties (e.g., negligible volatility, high stability, large liquidus range, tunable properties, etc.) [1–3]. The considerable utility of RTILs is manifested by an ever increasing number of reports concerning their use in synthesis [4–18], separation science [19–26], mass spectrometry [27–30], electrochemistry [31–34] and other diverse areas [35,36]. In many of these studies, the ionic liquids (and the results obtained therein) were compared and contrasted to those of more common molecular solvents. As a result of their increased use, efforts to better understand ionic liquids (ILs) and explain their actions became increasingly important. Early on it was noted that all ILs seemed to have polarities similar to propanol [1–3] and partitioning behavior similar to dipolar aprotic solvents or short chain alcohols [2,19]. However, it also was noted that this simple view was inadequate since different ILs having the same apparent polarity produced very different reaction rates, product ratios and yields when used in organic synthesis. Subsequently, it was found that ILs were better characterized by multiple solvation parameters [37].

Other observations concerning unusual and interesting solvation properties of ILs have been reported. For example, butylmethylimidizolium chloride (BMIM-Cl) was shown to dissolve up to 25% cellulose by Rogers and co-workers [38]. Solvophobic interactions between RTILs and dissolved surfactant molecules manifested themselves by lowering the surface tension of the RTIL solution and the apparent formation of micelles [39,40]. This implies that hydrocarbon chains in RTILs and water might behave in a somewhat analogous or related manner.

Not only are the number and variety of studies involving ILs increasing, but a number of new types of ILs are being developed as well. There is a growing need for a basic understanding of solvation by ILs. Such an understanding may allow for more efficient and effective design and utilization of ILs as well as provide other insights in to their properties. Currently, only a few empirical studies on solvation in/by ionic liquids have been reported. Electron paramagnetic resonance (EPR) was used to determine isotropic hyperfine coupling constants and g values of tempo and tempamine in a basic molten salt [41]. The fluorescent probe, coumarin 153,

A. Berthod (✉)
Laboratoire des Sciences Analytiques, CNRS, Université de Lyon 1, Bat. CPE, 69622 Villeurbanne, France
E-mail: berthod@univ-lyon1.fr

J. J. Kozak
Beckman Institute, California Institute of Technology, Pasadena, CA 91125-7400, USA

J. L. Anderson
University of Toledo, Department of Chemistry, Toledo, OH 43606, USA

J. Ding · D. W. Armstrong
University of Texas-Arlington, Department of Chemistry, Arlington, TX 76001, USA

was used to evaluate the solvation dynamics of several RTILs [42–47]. It was found that solvation was comprised of two time-resolved components. The physical origin of the two components stemmed from the polarizability of the organic cation (i.e., the faster component) and the slower relative diffusional motion of the cation and anion [47]. In other work, it has been noted that clathrate formation is common with ILs [48].

In this work, we measured the entropies and enthalpies of transfer between gas (alkanes) and liquid phases (ionic liquids above 80 °C) of a series of *n*-alkanes to ionic liquids using gas chromatography. A simple model that could account for the qualitative and quantitative experimental trends in very dilute solutions was derived and examined. Given the physicochemical behavior of alkanes and alkane containing solutes in ILs [39,40], we specifically choose an ordering phenomena model that is conceptually analogous to the effect found in dilute aqueous solutions of certain nonelectrolytes; nonpolar groups can adhere to one another in an aqueous environment (the hydrophobic effect), thereby changing the local ordering of the solvent [49,50]. Both the predicted enthalpies, entropies and their trends with increasing alkane molecular weight are compared with experimentally measured values. The model is then used in conjunction with the determined enthalpies with examine possible dielectric constants and inter-ionic distances of the RTILs.

2 Experimental

2.1 Chemicals

All chemicals were obtained from Aldrich (Milwaukee, WI) or Sigma (St. Louis, MO). They were of analytical grade and used as received. The ionic liquids were synthesized by simple reaction of methyl imidazole with butylhalide for 72 h at 70 °C. The triflate ionic liquid was formed by methylation of butylimidazole with methyltrifluoromethanesulfonate, and the hexafluorophosphate IL was obtained by metathesis of the 1-butyl-3-methylimidazolium chloride (BMIM-Cl) with hexafluorophosphoric acid. The RTIL synthesis was described in detail in recent works [19,37]. Table 1 lists some relevant properties of the RTILs used.

Table 1 Physico-chemical properties of the ionic liquid used in the study

Ionic liquid[a]	f.w. (Dalton)	m.p. (°C)	d ($g\,cm^{-3}$)	Anion diameter (Å)
BMIM-Cl	174.5	65	1.10	3.62
BMIM-Br	219.1	70	1.30	3.90
BMIM-I	265.9			4.32
BMIM-TfO	288	16	1.29	6.40
BMIM-PF_6	284	8	1.36	5.10
BMPy-NTf_2	418	−50	1.40	7.57

[a] $BMIM^+$ length: 11.0 Å, $BMIM^+$ width: 5.8 Å; $BMPy^+$ length: 11.1 Å, $BMPy^+$ width: 5.6 Å

2.2 Capillary columns

Six columns were prepared, for the inverse GC measurements on the RTILs, 250 µm i.d., polyimide coated silica capillary tubing (Supelco, Bellefonte, NJ) that was cut in 5-m pieces. The six 5-m capillary columns were statically coated with a 0.25% w/v dichloromethane solution of the six RTILs listed in Table 1. The full procedure was extensively described previously [37]. It produces columns evenly coated with a RTIL film of 0.12 µm thickness. The RTIL stationary phase mass and volume are, respectively, about 0.6 mg and 0.47 mm^3 per column. The column phase ratio (stationary phase volume over the mobile phase volume), $\phi 1$, is 1.9×10^{-3} (column volume is 245 mm^3 and Ln $\phi = -6.3$).

The stability of the six capillary columns was checked as follows: naphthalene was injected six times at a constant 100 °C temperature and at ∼8 h intervals. No changes in retention times as well as peak efficiency were noted with the six columns. This indicates that there is no measurable stationary phase bleed with the six ionic liquids tested.

2.3 Apparatus

A Hewlett Packard model 6890 gas chromatograph was used with a HP 6890 integrator. The carrier gas was helium used with an inlet column pressure of 0.2 $kg\,cm^{-2}$ or 3 psi. giving an average gas flow rate of 1 $mL\,min^{-1}$, average gas velocity of 30 $cm\,s^{-1}$ and an average dead time of 15–20 s. Split injections were required (split ratio of 50 to 1). A flame ionization detector was used. The injector and the detector were both set at 250 °C.

2.4 Protocol

The Gibbs free energy change of the solute between the mobile and the stationary phase, ΔG^o, is given by:

$$\Delta G^o = -RT \ln (k/\varphi), \tag{1}$$

where k is the solute retention factor and ϕ is the column phase ratio. The enthalpy, ΔH^o, and entropy, ΔS^o, are obtained from the change in the retention factor with temperature according to:

$$\ln k = -\Delta H^o/RT + \Delta S^o/R + \ln \varphi \tag{2}$$

Slopes and intercepts of the van't Hoff plots ($\ln k$ vs. $1/T$) will give the thermodynamic parameters of the solute's transfer from the gas phase to the ionic liquid stationary phase.

A total of 48 van't Hoff plots were made using eight test solutes [i.e., the linear even alkanes from octane (C8) to docosane (C22)] and six different ionic liquid columns (Table 1). All plots were linear in the 80–150 °C temperature range with regression coefficients equal to or higher than 0.995. As indicated previously, the advantage of using inverse GC to measure physico-chemical characteristics of ILs is that it is a highly temperature controlled environment in which volatile impurities (e.g., H_2O, CO_2, etc.) can be

excluded [37]. ILs are known to be hygroscopic and water is a well-known contaminant that significantly affects their properties. The hold-up times and/or volumes at all temperatures were determined by injecting methane.

The errors between the experimentally determined enthalpies and the theoretical model were determined according to the following equation:

$$\%\ \text{Error} = [100 - (\Delta H_{\text{Theoretical}}/\Delta H_{\text{Experimental}})^{*}100]$$

The experimentally determined enthalpy for one pair of ions was taken to be 44.6 kJ/mol^{-1} and that for the two pairs of ions was 86.1 kJ/mol^{-1} (see Results and discussion).

3 Results and discussion

3.1 Experimental results

The 48 van't Hoff plots were linear indicating that there is no state change neither in the solute gaseous state nor in the IL stationary phase in the liquid state over the 80–150 °C temperature range. Indeed, a change of state either of the solute or the stationary phase produces a characteristic break in the ln k versus $1/T$ plots [51]. Interfacial adsorptions between gaseous alkanes and ILs are the first step of the studied gas–liquid partitioning equilibrium. This initial adsorption is likely followed by transfer throughout the bulk IL liquid phase. The kinetic of this transfer will affect the peak widths but not the peak positions. The measured retention factors, k, are proportional to the thermodynamic distribution constants, K_D, of the gaseous alkane–liquid IL partition equilibrium.

Figure 1 shows plots of the enthalpies and entropies of transfer from the gas phase to six different ionic liquid phases (Table 1) for eight even n-alkanes (from C8 to C22). Three things are immediately obvious from this data: (1) there is very little difference in the enthalpies and entropies of transfer for a given n-alkane to different ionic liquids, (2) longer (larger) alkanes have more negative enthalpy and entropy values and (3) there is a linear relationship between the enthalpy and entropy values and the carbon number of the n-alkanes. Table 2 lists the average ΔH and ΔS for each of the eight n-alkanes, along with their various size parameters and densities.

The experimentally measured enthalpy changes are between −36.4 kJ mol^{-1} for octane and −86.1 kJ mol^{-1} for docosane. A linear relationship linking ΔH, the enthalpy variation, to n_C, the carbon number of the hydrocarbon alkyl chain, was found to be:

$$\Delta H = -3.51 n_C - 9.66 \quad (\text{in kJ mol}^{-1})$$
$$r^2 = 0.9974 \qquad (3)$$

The magnitude of the ΔS experimental values is between −65.5 J K^{-1} mol^{-1} for octane and −127.4 J K^{-1} mol^{-1} for docosane (Table 2). Similarly, a relationship linking ΔS, the entropy variation, to n_C was found as:

$$\Delta S = -4.25 n_C - 33.6 \quad (\text{in J mol}^{-1}\text{K}^{-1})$$
$$r^2 = 0.9957 \qquad (4)$$

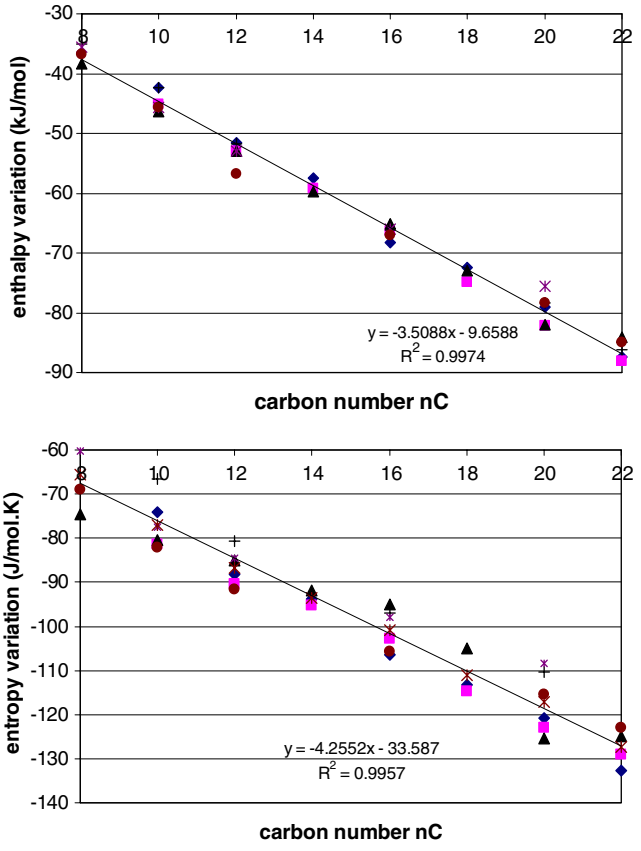

Fig. 1 *Top*, Enthalpy variation in kJ mol^{-1} obtained for the alkane test solutes. *Bottom* Entropy variation in J mol^{-1} K^{-1} . *Diamonds* BMIM Cl, squares BMIM Br, triangles BMIM I, *plus* BMIM PF_6, *Xs* BMIM TfO, *circles* BMPyr NTf_2. The *lines* are the average regression lines

Table 2 Enthalpy and entropy variations obtained experimentally by gas chromatography with ionic liquid stationary phases

Solute	f.w. (dalton)	Length (Å)	n_C	d(20°C) (g cm^{-3})	ΔH (kJ mol^{-1})	ΔS (J mol^{-1} K^{-1})
Octane	98	11.1	8	0.699	−36.4	−65.5
Decane	122	13.3	10	0.730	−44.6	−77.0
Dodecane	146	15.6	12	0.749	−53.2	−86.7
Tetradecane	170	18.0	14	0.763	−58.8	−93.7
Hexadecane	194	20.1	16	0.773	−66.5	−100.8
Octadecane	218	23.0	18	0.780	−73.5	−111.0
Eicosane	242	25.4	20	0.789	−79.3	−117.2
Docosane	266	28.0	22	0.794	−86.1	−127.4

The listed entropy and enthalpy values are the average values obtained on six different ionic liquid columns

The above two equations are valid for all six ionic liquids studied and they do not depend significantly on the anion nature and/or size.

3.2 Theoretical association model for ionic liquid–alkane systems

A simple, understandable model of hydrocarbon association with ionic liquids can be obtained using a Madelung-like

calculation (to describe the energetics) and simple combinatorial arguments (to understand the entropy trends). We are fully aware that a much more rigorous and sophisticated theory can, and should, be developed. However, a simple point of departure that provides a first-order understanding of the problem can be useful, particularly if it correlates with the experimental data and also triggers the interest of others in the field.

The impetus for this model was the experimental finding of an interesting entropy dependence in RTILs (Table 2). The model outlined here was a way of asking whether there was something akin to the "hydrophobic effect" at play in these systems [50]. Indeed, recent reports that normal micelles may form when surfactants are dissolved in RTILs, and that their occurrence is due to a "solvophobic effect" support this possibility [39,40]. The limitations of this model and possible directions for more inclusive and sophisticated theories are outlined at the end of this section.

The main hypothesis will be that the presence of an aliphatic chain disrupts the local structure of the ionic liquid, and induces a systematic ordering of positive and negative ions along the length of the solute alkyl chain. Furthermore, on energetic grounds, it will be shown that the ordering of pairs of ions is the preferred configuration. Such ordering has an immediate consequence in regard to the entropic, as well as enthalpic, behavior of the system.

3.2.1 Entropy

Figure 2 shows an idealized representation of the ordering of successive ionic liquid ion pairs along the hydrocarbon backbone of an alkane solute. This model can be used to evaluate the entropic changes induced by such an arrangement. The basic conclusion drawn from the energetic (enthalpy) analysis is that the most favorable configurations are those in which a first cation/anion pair is aligned, then a second cation/anion pair, then a third pair, etc... (see following section). To realize the first cation/anion configuration (Fig. 2, top), either the cation or anion can, in principle, be localized first. So, initially, one has two choices. But, once the first ionic species is chosen, the partner must be oppositely charged. Thus, the number W of possible arrangements for the first ion pair is:

$$W = (2)(1) = 2 \tag{5}$$

If one now considers the alignment of two ion pairs as shown by Fig. 2 (middle), one of four ions should be picked first. If a cation is chosen, then the next ionic species must be an anion, of which there are two possibilities. Finally, energetically, the next ion must be the remaining cation and the remaining anion terminates the two ion pair arrangement. Overall, then, the W number for two ion pairs, noted $W(2)$ is:

$$W(2) = (4)(2)(1)(1) = 8 \tag{6}$$

Following the same line of reasoning, the alignment of three ion pairs (Fig. 2, bottom) shows that there are six possible choices for the first ion. Then, there are three choices for the next ion that must be of opposite charge. To align the second ion pair, there are two possible choices for the next cation and also two possible choices for the partnering anion. And, for the last ion pair, there is only one possible choice for the next cation and remaining anion. Overall, then, the W number is:

$$W(3) = (6)(3)(2)(2)(1)(1) = 72 \tag{7}$$

Considering a few more examples allow one to deduce the following general expression:

$$W(n) = n^2 W(n-1) = 2\prod_{i=1}^{n} i^2 \tag{8}$$

Table 3 lists the $W(n)$ values up to nine ion pairs.

Using the classical Boltzman thermodynamic relation between the number $W(n)$ of possible arrangements and the entropy,

$$S(n) = k \ln W(n) \tag{9}$$

the entropy $S(n)$ can be calculated as a function of the number n of ion pairs aligned on the hydrocarbon backbone. The

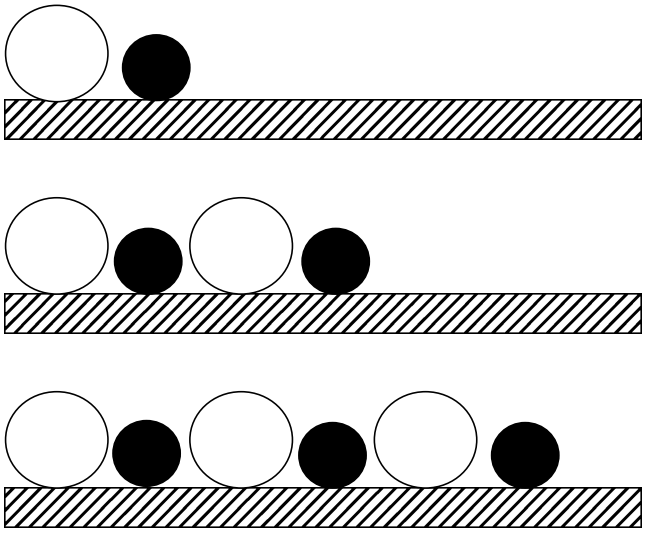

Fig. 2 An idealized representation of the ordering of successive ionic liquid ion pairs along the hydrocarbon backbone of an alkane solute (*dashed bar*). The *open circles* represent the cations and the *black circles* represent the anions

Table 3 Calculated entropy changes according to Eq. (11) (in J K^{-1} mol^{-1})

Ion pairs	W(n) $n^2 W(n-1)$	R Ln $W(n)$ (J K^{-1} mol^{-1})	R Ln $(2n)!$ (J K^{-1} mol^{-1})	ΔS (J K^{-1} mol^{-1})
1	2	5.8	5.8	0.0
2	8	17.3	26.4	−9.1
3	72	35.5	54.7	−19.2
4	1,152	58.6	88.1	−29.5
5	28,800	85.3	125.5	−40.2
6	1,036,800	115.1	166.1	−51.0
7	50,803,200	147.4	209.3	−61.9
8	3,251,404,800	182.0	254.0	−72.9
9	2.63364×10^{11}	218.5	302.4	−83.9

reference state is specified for the case where the cations and the anions are discharged, and both species can be laid down randomly along the alkyl chain. The associated entropy in this case is given by the standard expression for $2n$ indistinguishable particles, viz.,

$$S_o = k \ln (2n)! \tag{10}$$

Thus, relative to this reference state and on a molar basis, the change in entropy is given by:

$$\Delta S = R[\ln W(n) - \ln (2n)!] \tag{11}$$

R being the gas constant ($R = kN$).

To get a sense if the analytic dependence of the entropy variation is a function of the number (n) of associated pairs of ions, one can use Stirling's approximation to simplify Eq. (11) to read:

$$\Delta S \approx -2R\, n \ln 2n + R\left[\ln 2 + 2\sum_{i=1}^{n} \ln i\right] \tag{12}$$

As is evident, the model predicts that the change in entropy should decrease almost linearly with n (with high n values). For the initial n values, one can compute the exact slope from the theoretical data listed in Table 3 (without Stirling's approximation), and the result ($1 \leq n \leq 9$) is -10.6 J/K mol entropy change per additional ion pair with a regression coefficient 0.9994.

3.2.2 Enthalpy

Considering the scheme shown in Fig. 2, cations repel each other and attract anions according to Coulomb's law:

$$\text{Force} = \frac{1}{4\pi\varepsilon_o\varepsilon}\frac{(+ze)(+z'e)}{a^2}, \tag{13}$$

where z is the valence of the ions, e the basic unit of charge (1.6×10^{-19} C), a the separation between the two ions (in m), ε is the dielectric constant factor ($\varepsilon = 1$ in vacuo), ε_o is the permittivity of free space ($8.8542 \times 10^{-12}\,\mathrm{C^2\,N^{-1}\,m^{-2}}$) and the constant term $1/4\pi\varepsilon_o$ is $9 \times 10^9\,\mathrm{N\,m^2\,C^{-2}}$.

The dielectric constant, ε, is the physico-chemical parameter indicating the magnitude of the decrease of the Coulombic attraction due to the medium. It may be surprising to evoke a dielectric constant in an ionized medium such as an ionic liquid. For reference, typical dimensionless dielectric constants ε, for some typical liquids, solids and gases are listed in Table 4. It is well-known that the dilute state of gases (20°C and 1 atm) do not appreciably decrease the Coulombic attraction of ions, whereas liquids with a strong dipole moment can decrease this attraction by two orders of magnitude (hydrogen cyanide, *N*-methylformamide). The dielectric constant of solid salts is often around 10 (Table 4).

The Coulombic energy is the product of the force times the separation distance between two ions

$$\text{Energy} = \frac{zz'}{4\pi\varepsilon_0\varepsilon}\frac{ee'}{a}. \tag{14}$$

Table 4 Dielectric constants of selected compounds at 293 K

Compound	ε	Compound	ε
Gas			
Nitrogen	1.0004	Methane	1.0008
Oxygen	1.0005	Propane	1.0019
Liquids			
Hexane	1.89	Pyridine	13.3
Hydrogen chloride (−15 °C)	6.35	Sulfur dioxide	16.3
Chloroform	4.81	Dimethylsulfoxide	47.2
1-octanol	10.3	Acetamide	67.6
1-propanol	20.8	Water	80.1
Ethanol	25.3	Formamide	111
Methanol	33.0	Hydrogen cyanide	115
Methylisobutyl ketone	13.1	*N*-methylformamide	189
Solids			
NaCl	5.9	AgCl	11.1
CsCl	6.3	$BaSO_4$	11.4
NH_4Cl	6.9	$PbSO_4$	14.3
$NaNO_3$	6.85	$TlNO_3$	16.5

Data from D.R. Lyde, Handbook of Chemistry and Physics, CRC Press, 81st (ed), (2000)

Following the logic of a classical Madelung-constant calculation [52–54], it is assumed that a cation is localized in the immediate neighborhood of the hydrocarbon chain and a second ion moves into the vicinity. If this second ion is another cation, the Coulombic energy will be positive, i.e., repulsive, and this pairing will not be stable. If the second ion is an anion, the configuration will be stabilized by an energy E

$$E_{1,2} = \frac{-zz'}{4\pi\varepsilon_0\varepsilon}\frac{e^2}{a} \tag{15}$$

since all the ionic liquid ions have the same charge (Fig. 2 top).

The question now arises as to what happens when a third ion is added to this system. In the linear array shown in Fig. 2 (middle), that ion would be a second cation. Hence, relative to the first pair of ions, the Coulombic energy of the addition of this single ion to the existing pair would be

$$E_{1,3} = \frac{-zz'}{4\pi\varepsilon_0\varepsilon}\left(\frac{e^2}{a} - \frac{e^2}{2a}\right) = \frac{-zz'}{4\pi\varepsilon_0\varepsilon}\frac{e^2}{2a}. \tag{16}$$

Bringing a second anion to complete the configuration, making two pairs of ions as displayed in Fig. 2 (middle), the energy for the incoming second anion would be

$$\begin{aligned} E_{1,4} &= \frac{-zz'}{4\pi\varepsilon_0\varepsilon}\left(\frac{e^2}{a} - \frac{e^2}{2a} + \frac{e^2}{3a}\right) \\ &= \frac{-zz'}{4\pi\varepsilon_0\varepsilon}\frac{e^2}{a}\left(1 - \frac{1}{2} + \frac{1}{3}\right) = \frac{-zz'}{4\pi\varepsilon_0\varepsilon}\frac{e^2}{a}(0.8333\ldots). \end{aligned} \tag{17}$$

The point to note is that bringing a single ion to a pre-existing pair is less energetically favorable than complementing the first pair of ions with a second pair.

This trend continues as more ions are added. Table 5 lists the energy needed to bring more ions one after the other.

Table 5 Energy in units of $(-z^2e^2/4\pi\varepsilon_o\varepsilon a)$ needed to bring successive ions along the hydrocarbon chain

Ion number	Coefficient for the nth ion	Cumulative energy
2	1	1 (1 ion pair)
3	0.5	
4	0.8333...	2.333... (2 ion pairs)
5	0.5833...	
6	0.7833...	3.7 (3 ion pairs)
7	0.6166...	
8	0.75982	5.076... (4 ion pairs)
...		
∞	Ln 2 = 0.69315	

The energy term, $E_{1,n}$, for n ions can be expressed by the summation:

$$E_{1,n} = \frac{-zz'}{4\pi\varepsilon_0\varepsilon}\frac{e^2}{a}\sum_{i=1}^{n-1}\frac{(-1)^{i+1}}{i} \tag{18}$$

which converges to $-\ln 2zz'e^2/(4\pi\varepsilon_o\varepsilon a)$or $-1.6\times10^{-28}/(\varepsilon a)$J.

Since we have now shown that the energetically-preferred organization of ions along the one-dimensional aliphatic chain is n ion-pairs ($2n$ ions), we can now proceed to calculate the total Coulombic energy (E_T) of a given array, viz.

$$E_T = \sum_{i=2}^{2n} E_{1,i} \tag{19}$$

The energy for one pair of ions is expressed by Eq. 15. With two pairs of ions (Fig. 2, middle), the total energy is

$$\begin{aligned} E_{1,n} &= \{E_{12}+E_{13}+E_{14}+E_{23}+E_{24}+E_{34}\}\text{ or}\\ E_{1,n} &= \tfrac{-zz'}{4\pi\varepsilon_0\varepsilon}\tfrac{e^2}{a}\{2.333\ldots\} \end{aligned} \tag{20}$$

Similarly, with three pairs of ions (Fig. 2, bottom), it is

$$E_{1,n} = \frac{-zz'}{4\pi\varepsilon_0\varepsilon}\frac{e^2}{a}\{3.7\}. \tag{21}$$

The successive coefficients for additional pairs can be calculated as 5.076, 6.456 and 7.839, for 4, 5 and 6 ion-pairs respectively, clearly showing a linear decrease in E_T with increase in the number of pairs associated with the alkyl chain (Table 5). This energy change is directly related to the enthalpy change, ΔH, associated with alkane-ionic liquid solvatation, and can be correlated with the experimentally derived values and trends.

3.3 Entropy changes

The experimental entropic change has a slope of $-4.25\,\mathrm{J\,K^{-1}\,mol^{-1}}$ per carbon atom (Fig. 1 and Eq. 4). The one dimensional theoretical model predicts a linear decrease of ΔS with the number of ionic liquid ion pairs associated with the alkane and a slope of $-10.6\,\mathrm{J\,K^{-1}\ mol^{-1}}$ per ion pair (Eq. 12). This discrepancy can be resolved by slightly altering (or making an addition to) the simple model as shown in Fig. 3, where

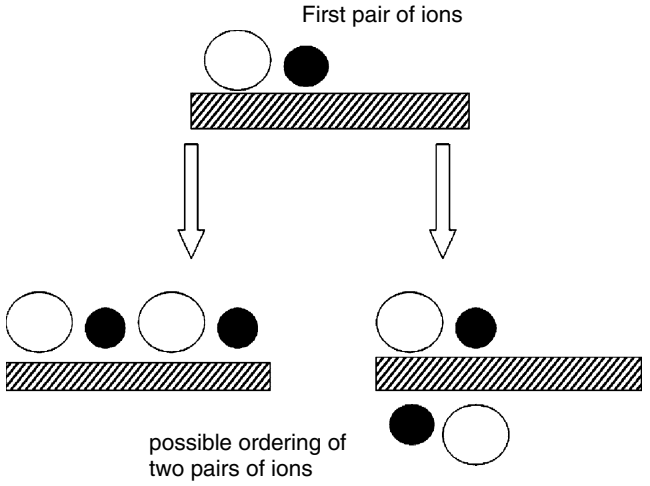

Fig. 3 For entropic purposes, it is necessary to take into account the fact that the pairs of ions can be aligned on the same side or the opposite side of the alkane (as shown). As noted in the text, the accurate calculation of ΔS requires that this type of ordering be accounted for

an additional pair of ions can be aligned either linearly on the same side of the alkane, or on the opposite side of the alkane. While the energy of both configurations is similar, the entropy is not. Overall, the combinatorial factor for this second scenario is:

$$W(n) = n^2\{2^{n-1}\}W(n-1) \tag{22}$$

If one now proceeds in the same way (as in Table 3) to calculate the slope (ΔS), a result of $-4.8\,\mathrm{JK^{-1}\,mol^{-1}}$ (slope 0.997) is obtained instead of $-10.7\,\mathrm{JK^{-1}\,mol^{-1}}$. The later value is quite close to the experimental one.

Qualitatively, then, the decrease in ΔS with increase in alkane chain length, as experimentally obtained and documented in Table 3, is consistent with the representation diagrammed in Fig. 3, whereby an increase in chain length can be accompanied by an increased number of paired ions associated with an n-alkane. As mentioned by Franks, 40-years-ago for alkanes and water, inert alkane molecules could promote the structuring of the neighboring solvent ion pairs [50].

3.4 Enthalpy changes

The experimentally measured enthalpies, and their trends for the homologous series of n-alkanes, can be compared with the values and trends predicted by the simple Coulombic model (Eq. 18), provided the dielectric constant (ε) and the interionic distance (a) of the ionic liquids are known. Conversely, Eq. 18 can be used in conjunction with the experimentally measured enthalpies to estimate values of (ε) and (a) for the ionic liquid. The number of ion pairs directly associated with the n-alkane (Fig. 3) provides the coefficient needed to calculate the energy values of interest. By picking a reasonable series of (a) and (ε) values that are likely to span the actual values, a series of enthalpies can be calculated for any number of paired ions. This was done and the results are given in

Table 6 Calculated enthalpy changes according to Eq. 17 (in kJ mol^{-1})

Dielectric constant, ε	1	4	10	10	13.5	16	10	20	
Distance, a (nm)	4	1	0.5	0.35	0.3	0.25	0.2	0.2	
Number of ion pairs, n	Coefficient				E (kJ mol^{-1})				
1	1	−34.6	−34.6	−27.7	−39.6	−34.2	−34.6	−69.3	−34.6
2	2.33	−80.8	−80.8	−84.6	−92.3	−79.8	−80.8	−161.6	−80.8
4	5.076	−175.8	−175.8	−140.6	−200.9	−173.6	−175.8	−351.5	−175.8
6	7.839	−271.4	−271.4	−217.2	−310.2	−268.1	−271.4	−542.9	−271.4

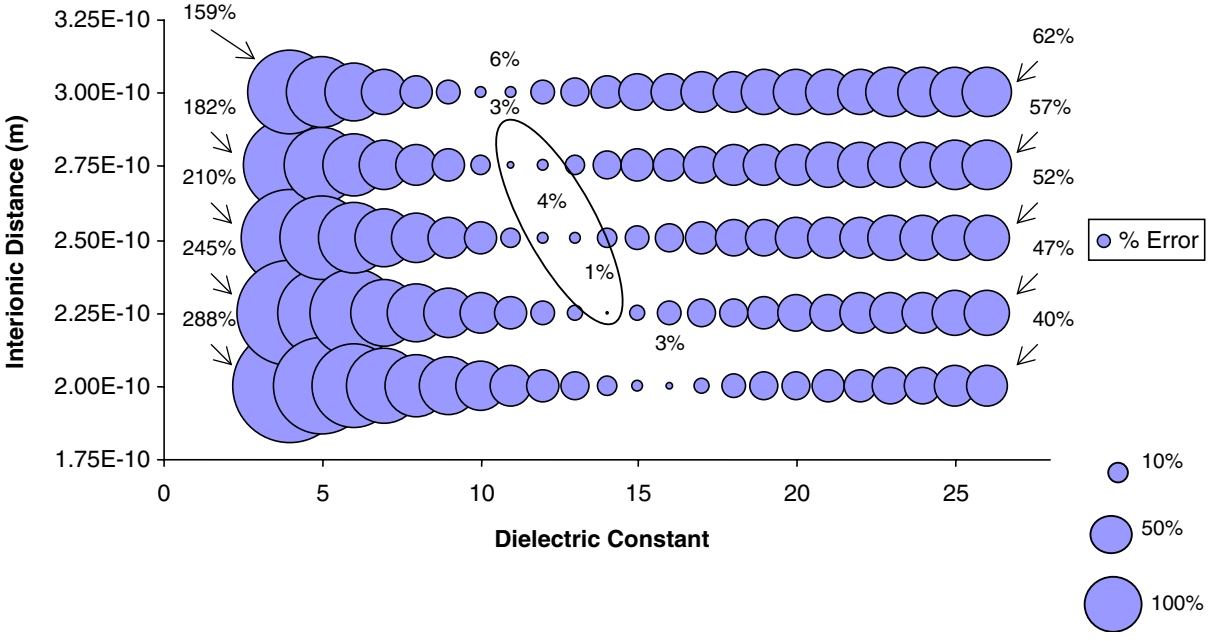

Fig. 4 Bubble plot comparing the experimental and predicted enthalpies of association (see text) required to form one ordered ion pair of an ionic liquid cation and anion next to an alkane molecule as a function of the dielectric constant (ε) and interionic distance (a). The magnitude of the interionic distance is expected to be slightly larger than that determined by X-ray crystallography ($a > 0.2$ nm). The error associated with comparing the experimental value for the enthalpy of association for one ion pair (44.6 kJ mol^{-1}) to the theoretical model is illustrated by the size of the circle in the plot (see bottom right hand corner for legend) and was calculated as described in the *Experimental*. The *smallest circles* ($\sim$ 4–8%) in which the experimental and theoretical values closely match occur with a dielectric constant range of $11 < \varepsilon < 15$ and an interionic distance of 2.1 Å < a < 2.7 Å

Table 6. The first thing that should be noted about this series of calculated enthalpies is that all the trends are identical. That is, the model predicts that all enthalpies become more negative when the number of associated paired ions increases (i.e., more ions associate with longer alkyl chains) and this same trend is found experimentally (Table 2 and Fig. 1). The second point to be noted is that the same magnitude ΔHs can be obtained for different values of (ε) and (a). This can happen when the (ε) and (a) values are directly transposed (Table 6 gives one example of this). However, as is noted in the following paragraph, only a narrow range of (ε) and particularly (a) values are possible.

Low temperature crystal structures (and/or Raman studies) have been reported for BMIM-Cl and BMIM-Br [55–57]. The minimum interionic distance for these solids is approximately 0.2 nm. Hence, it can be assumed that 0.2 nm < a < $\sim$0.4 nm is a realistic range for typical ionic liquids.

The number of ions (pairs of ions) that can solvate an n-alkane is limited by geometrical constraints. Table 2 gives the extended chain lengths of the n-alkanes. Table 1 gives the dimensions (lengths, widths and diameters) of the ions that comprise the various ILs. The length of the IL cation is similar to that of octane. Its width is about half its length. Hence, depending on its orientation, the BMIM cation would contact between $\sim$0.5 to a little more than 1.0 nm of an n-alkane (between $n_c = 4$ and $\sim n_c = 8$). The anion (except for NTf_2) would occupy somewhat less space ($\sim n_c = 3$ or $\sim$0.5 nm). Therefore, a pair of IL ions next to an n-alkane could occupy a distance as little as $\sim$1.07 nm ($n_c \sim 8$) to as much as $\sim$1.6 nm ($n_c \sim 12$) depending on whether the cation lies lengthwise or widthwise (note that these distances include a 0.2 nm interionic space).

Limits as to the IL's dielectric constants are probably within the range of values for known liquids and solid salts (Table 4). However, even this rather large range (i.e., hexane = 1.89 and N-methylformamide = 189) can be somewhat narrowed given the fact that ILs are molten salts (solid salts range from $\varepsilon \sim 4$ to 20) and have apparent polarities similar to short chain alcohols [19] (ε $\sim$10–33) (see Table 2).

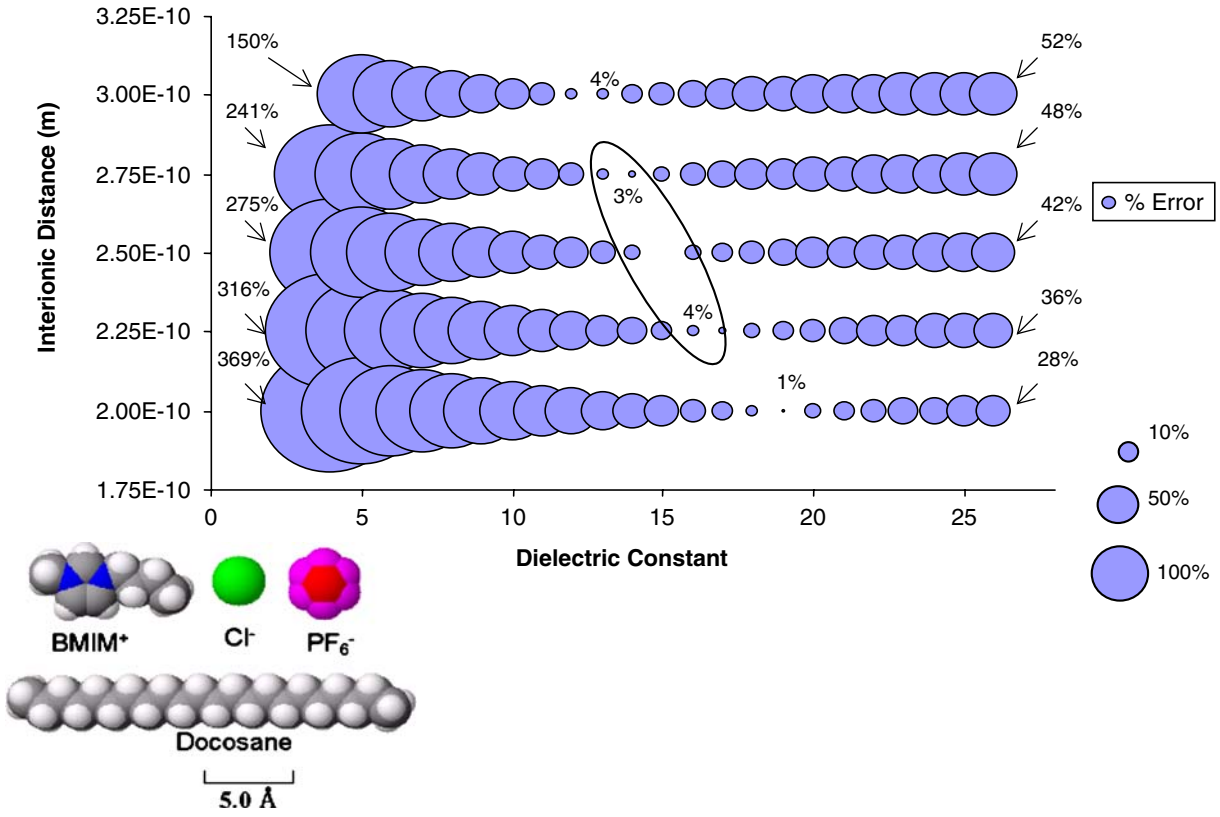

Fig. 5 Bubble plot comparing the experimental and predicted enthalpies of association (see text and Fig. 4 caption) required forming two ordered pairs of ions. The error associated with comparing the experimental value for the enthalpy of association for two ion pairs (86.1 kJ mol^{-1}) to the theoretical model is illustrated by the size of the circle in the plot (see bottom right hand corner for legend) and was calculated as described in the *Experimental*. The *smallest circles* (∼4–8%) in which the experimental and theoretical values closely match occur with a dielectric constant range of $13 < \varepsilon < 17$ and an interionic distance of 2.1 Å < a < 2.7 Å. The molecular model of the ions and longest tested molecule (C22) are shown at the bottom of the figure all at the same scale

Equation 18 can be used in conjunction with the experimentally measured enthalpies (Table 2) in order to evaluate the most likely interionic distances and dielectric constants for these ILs. We utilize the previously discussed dimensions of the ILs and the *n*-alkanes to determine the possible number of paired ions in the immediate vicinity of a given length *n*-alkane. Within these limits, the percentage error or difference between the theoretically predicted enthalpy and those determined experimentally can be determined for any selected values of (a) and (ε), see Experimental Section for the calculation. This was done and typical results for one pair and two pairs of ions solvating an *n*-alkane are shown in Figs. 4 and 5, respectively. Note that in both cases, there is a similar minimum error/difference between the theoretical and experimental enthalpies near the optimum values of (a) and (ε) (which are circled in Figs. 4, 5). Using this data the average ionic liquid's dielectric constant (ε) is ∼13.5 and the average interionic distance is ∼0.25 nm (2.5×10^{-10} m). Also, note that similar minimum errors can be obtained using other values of (a) and (ε). However, these can be easily excluded when those values are beyond the range of possibility (*vide supra*). For example, interionic distances of less than 0.2 nm can give an equally small error if a high enough (ε) is used. But, since 0.2 nm is the minimum interionic distance in the crystalline solid, it is not likely to be less for the molten IL. We are well aware that this simple Coulombic model, for the energetics of this system, does not take into account van der Waals forces or induced dipole interactions between the IL and alkane. Undoubtedly, these interactions are operative and also scale linearly with alkane chain length.

4 Conclusions

The interaction of *n*-alkanes with room temperature ionic liquids can be modeled using the ordering of the IL solvent along the extended hydrocarbon in a manner conceptually similar to that, which occurs in an aqueous solution of nonelectrolytes [49]. However, there are specific differences. For example, it is energetically and entropically favorable for ILs to interact as pairs of ions (Fig. 2). Indeed simple expressions were derived, based on this model, that allow calculation of ΔS_s and ΔH_s that are comparable in magnitude and trend to experimentally measured values. Both the enthalpy and entropy become more negative as the chain length of the alkane increases. There is little difference among the ILs

tested, in their solubilization behavior toward the *n*-alkanes at very low concentration. Using both the experimentally determined enthalpy and the theoretical expression for solvation energy, the dielectric constant and interionic distance for the studied ILs were estimated to be approximately 13.5 and 0.25 nm, respectively.

The outlined theory (in which the energetics are based on Coulombic interactions) does not adequately take into account van der Waals forces or ion induced dipole interactions between the ionic liquid and alkane. These interactions can contribute to the energetics of the system, and would also be expected to scale linearly with alkane chain length. Rather, this simple model describes an entropically driven system, somewhat analogous to an alkane interacting with water, where the solvent is forced to order itself around a solute that would prefer to isolate or exclude. In addition, the theory described here is based on a simple one-dimensional model when physically, the system of ions and chains is of dimension $D = 2$ (adsorption) or even 3 (solvation). However, what has been shown is that the essential behavior can be extracted from a model which is of mathematical dimension $D = 1$. Ultimately, a three dimensional (3D) model would be preferred.

Future alternative theoretical approaches/models of alkane-IL interactions could involve formation of a cavity in the IL, followed by insertion association with the alkane [58]. Undoubtedly, this and other more sophisticated theories/models will follow. It is hoped that the simplicity of the current model and its ability to describe the experimental gas chromatography results will provide an impetus for other theorists to become engaged in this area and provide a more comprehensive understanding of the problem.

Acknowledgements This research was supported by National Institutes of Health Grant – NIH R01 430-21-23. AB thanks the Centre National de la Recherche Scientifique UMR5180 (P. Lanteri) for continuous support.

References

1. Rogers RD, Seddon KR, (eds) (2002) Ionic liquids industrial applications to green chemistry. ACS Symporium Ser. 818. American Chemical Society, Washington
2. Wasserscheid P, Welton T, (eds) (2002) Ionic liquids in synthesis. Wiley-VCH Verlag Gmbh & Co., Weinhelm
3. Rogers RD, Seddon KR, (eds) (2002) Ionic liquids as green solvents progress and prospects. ACS Symposium Series 856. American Chemical Society, Washington
4. Wilkes JS, Zaworotko MJ (1992) J Chem Soc Chem Commun 965
5. Suarez PAZ, Dullius JEL, Einloft S, DuSouza RF, Dupont J (1996) Polyhedron 15:1217
6. Huddleston JG, Willauer HD, Swatloski RP, Visser AE, Rogers RD, Chem Commun 1765
7. Bonhote P, Dias AP, Papageorgiou N, Kalyanasundaram K, Gratzel M (1996) Inorg Chem 35:1168
8. Welton T (1999) Chem Rev 99:2071
9. Kim HS, Kim YJ, Lee H, Park KY, Lee C, Chin CS (2002) Angew Chem Int Ed 41:4300
10. Lozano P, De T, Diego Carrie D, Vaultier M, Iborra JL (2002) J Mol Catal B 21:7
11. Sheldon, RA, Chem. Comm. (2001) 2399
12. Wasserscheid P, Keim W (2000) Angew Chem Int Ed Engl 39:3772
13. Sheldon RA, Lau RM, Sorgedrager MJ, van Rantwijk F, Seddon KR (2002) Green Chem 4:146
14. Earle MJ, McCormac PB, Seddon KR (1999) Green KR, Chemistry 1:23
15. Wasserscheid P, Bosmann A, Bolm C (2002) Chem Commun 200
16. Ishida Y, Miyauchi H, Saigo K (2002) Chem Commun 2240
17. Ding J, Desikan V, Han X, Xiao TL, Ding R, Jenks WS, Armstrong DW (2005) Org Lett 7:335
18. Pegot B, Thanh G, Gori D, Loupy A (2004) Tetrahedron Letters 45:6425
19. Carda-Broch S, Berthod A, Armstrong DW (2003) Anal Bioanal Chem 375:191
20. Dai S, Ju YH, Barnes CE (1999) J Chem Soc Dalton Trans 1201
21. Visser AE, Swatloski RP, Reichert WM, Mayton R, Sheff S, Wierzbicki A, Davis JH, Rogers RD (2001) Chem Commun 135
22. Chun, S, Dzyuba, SV, Bartsch, RA, Anal. Chem. 73 (2001) 3737
23. Armstrong DW, He L, Liu LS (1999) Anal Chem 71:3873
24. Berthod A, He L, Armstrong DW (2001) Chromatographia 53:63
25. Anderson JL, Armstrong DW (2003) Anal Chem 75:4851
26. Ding J, Welton T, Armstrong DW (2004) Anal Chem 76:6819
27. Armstrong DW, Zhang LK, He L, Gross ML (2001) Anal Chem 73:3689
28. Carda-Broch S, Berthod A, Armstrong DW (2003) Rapid Commun Mass Spectrom 17:553
29. Mank M, Stahl B, Boehm G (2004) Anal Chem 76:2938
30. Li YL, Gross ML (2004) J Am Soc Mass Spectrom 15:1833
31. Dickenson VE, Williams ME, Hendrickson SM, Masui H, Murray RW (1999) J Am Chem Soc 121:613
32. Bhatt AI, May I, Volkovich VA, Hetherington ME, Lewin B, Tied RC, Ertok N (2002) J Chem Soc, Dalton Trans 4532
33. Lagrost C, Carrie D, Vaultier M, Hapiot P (2003) Phys J, Chem A 107:745
34. Leone AM, Weatherly SC, Williams ME, Thorp HH, Murray RW (2001) J Am Chem Soc 123:218
35. Ue M, Takeda M, (2002) J Korean Electrochem Soc 5:192
36. Wang P, Zakeeruddin SM, Comte P, Exnar I, Gratzel M (2003) J Am Chem Soc 125:1166
37. Anderson JL, Ding J, Welton T, Armstrong DW, (2002) J Am Chem Soc 124:14247
38. Swatloski RP, Spear SK, Holbrez JD, Rogers RD (2002) J Am Chem Soc 124:4974
39. Anderson JL, Pino V, Hagberg EC, Shears VV, Armstrong DW (2003) Chem Comm 2444
40. Fletcher KA, Pandey S (2004) Langmuir 20:33
41. Noel MAM, Allendoerfer RD, Osteryoung RA (1992) J Phys Chem 96:2391
42. Karmakar R, Samanta A (2002) J Phys Chem A 106:4447
43. Karmakar R, Samanta A (2003) J Phys Chem A 107:7340
44. Ingram JA, Moog RS, Ito N, Biswas R, Marancelli M (2003) J Phys Chem B 107:5926
45. Chakrabarty D, Hazra P, Chakrabarty A, Seth D, Sarkar N (2003) Chem Phys Lett 381:697
46. Arzhantsev S, Ito N, Heitz M, Maroncelli M (2003) Chem Phys Lett 381:278
47. Chowdhury PK, Halder M, Sanders LE, Calhoun T, Anderson JL, Armstrong DW, Song X, Petrich JW (2004) J Phys Chem B 108:10245
48. Holbrey JD, Reichert WM, Nieuwenhuyzen M, Sheppard O, Hardacre C, Rogers RD (2003) Chem Comm 476
49. Kozak JJ, Knight WS, Kauzmann J (1968) J Chem Phys 48:675
50. Franks F (1974) Water. A Comprehensive Treatise. Plenum Press, New York vol 4, Chapter 1, pp 1–94
51. Rayss J, Patrykiejew A Serpinet J (1989) Thin Solid Films 173:13
52. Flory PJ (1942) Chem Phys 10:51
53. Huggins ML (1942) Ann Acad NY Sci 43:1
54. Moelwyn-Hugues EA (19957) Physical Chemistry. Pergamon Press, London pp 543
55. Katayanagi H, Hayashi S, Hamagushi H, Nishikawa K (2004) Chem Phys Lett 392:460
56. Holbrey JD, Reichert WM, Nieuwenhuyzen M, Johnston S, Seddon KR, Rogers RD (2003) Chem Comm 1636
57. Saha S, Hayashi S, Kobayashi A, Hamagushi H (2003) Chem Lett 32:740
58. Glesen DJ, Cramer CJ, Truhlar DG (1995) J Phys Chem 99:7137